

CubeSat in-orbit validation of in-situ performance by high fidelity radiation modelling

Arpad Lenart,^{*} Bernhard Hidding,[†] and Daniel K. L. Oi[‡]
SUPA Department of Physics, University of Strathclyde, Glasgow G4 0NG, United Kingdom

Srihari Sivasankaran[§] and Alexander Ling[¶]
Center for Quantum Technologies (CQT), National University of Singapore (NUS)

Peter Neilson^{**}
Tech-X Corporation
 (Dated: September 2, 2022)

Abstract: Space based quantum technologies are essential building blocks for global quantum networks. However, the optoelectronic components and devices used are susceptible to radiation damage. The SpooQy-1 CubeSat mission demonstrated polarization-based quantum entanglement correlations using avalanche photodiodes for single-photon detection. We report the increasing dark count rates of two silicon Geiger-mode avalanche photodiodes (GM-APD) observed throughout its 2 year orbital lifetime. As a means of diagnosing the unexpected trends in the increase of dark counts, we implement a high-fidelity radiation model combined with 3D computer aided design models of the SpooQy-1 CubeSat to estimate the accumulated displacement damage dose in each photodiode. Using these results, we were able to support the claim that differences in radiation shielding was a major contributor to the observed in-orbit data. This illustrates how radiation modelling can have applications beyond conventional lifetime estimates for low-earth orbit CubeSats.

Keywords: Radiation modelling, displacement damage dose, avalanche photodiodes, dark counts

I. INTRODUCTION

The democratization of space access, often dubbed New Space, has opened up the potential of low cost missions utilizing commercial off the shelf (COTS) components. While a burgeoning market for small satellite platform systems has developed, CubeSats in particular, payloads may require the use of non space grade devices and sub-systems. Whilst testing and qualifying these for vibration, thermal, and vacuum conditions is relatively well established, testing instruments for radiation induced damage remains less representative and amounts to a source of high uncertainty for satellite missions [1]. Even if radiation tolerance of a component is known, this information needs to be combined with measurements, or predictions of its exposure to the types, levels, and energy distribution of radiation.

Space radiation in general occurs due to highly energetic particles like electrons, protons, ions, and neutrons. Radiation damages can be categorized as Single event effects and Cumulative effects. Cumulative radiation damages are further subcategorized as Total Ionizing Doses (TID) and Displacement Damage Doses (DDD) [2]. Here, we primarily focus on the cumulative radiation doses that cause the circuits' gradual performance deterioration.

The radiation-induced performance degradation is not always well understood for COTS devices which are not radiation hardened by design, hence the observed degradation may vary significantly on a part-to-part basis [1]. Nevertheless, using the radiation modelling of the satellite and its environment the radiation exposure of instruments still need to be simulated and compared with radiation tests. This forms the primary means by which in-orbit performance can be assured.

While radiation models are conventionally used for lifetime predictions, here, we investigate the extent to which we can use it to predict radiation-induced performance degradation over time. We apply high-fidelity radiation modelling techniques to the SpooQy-1 CubeSat space mission and correlate this to real-time in-orbit measurements as an attempt to diagnose unexpected instrument behavior. This involves the use of a time-varied mission based radiation fluences predicted by SPENVIS (Space Environment Information System) [2] combined with detailed computer aided design (CAD) models of the SpooQy-1 CubeSat. The radiation effects on the Silicon Avalanche Photodiodes (APDs) onboard the CubeSat are simulated using Monte Carlo Geant4-based radiation software RSim [3, 4]. This model predicted that we should expect 58% (+ 31%) increased radiation damage in one of the APDs which correlated well with in-situ measurements. A detailed analysis was completed to ensure the performance degradation was infact radiation induced, while the part-to-part variability in APD behavior may be a contributor, the agreement with simulated radiation effects and in-situ performance measurements suggest that this behavior is likely owed to varied shielding levels due to the internal CubeSat structure.

^{*} arpad.lenart@strath.ac.uk

[†] bernhard.hidding@strath.ac.uk

[‡] daniel.oi@strath.ac.uk

[§] srihari@speqtral.space

[¶] alexander.ling@nus.edu.sg

^{**} neilson@txcorp.com

II. BACKGROUND

A. SpooQy-1's Space Mission

The SpooQy-1 is a 3U CubeSat deployed into orbit from the International Space Station on 19th June 2019 with operations conducted from Switzerland and Singapore ground stations [5]. It features an entangled photon source and single photon detection system with measurements of polarization entangled photons performed routinely and successfully since launch and deorbited in late 2021. The primary objective of SpooQy-1 was to demonstrate polarization based quantum entangled-photon pair source in space environment. This would set the pathway for future missions with quantum technologies, towards building global quantum networks.

The Center for Quantum Technologies (CQT) at the National University of Singapore (NUS) developed the payload Small Photon Entangling Quantum System (SPEQS-2) for the SpooQy-1 mission, which by itself is the second iteration of the system, designed to demonstrate entanglement-based Quantum Key Distribution (QKD) in space environment. QKD networks enable a more secure communication between two parties, involving the exchange of individual entangled photon pairs and uses their quantum states to encode information. Demonstrating this using miniaturized systems builds confidence in QKD technology and increases its technological readiness level.

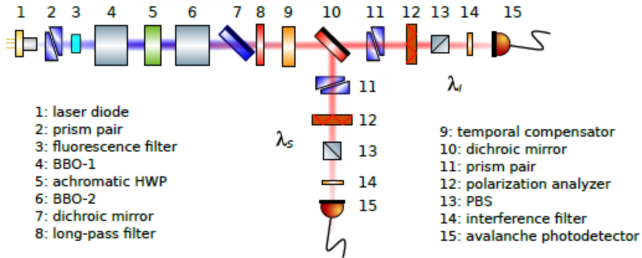


FIG. 1. Optical layout of the SPEQS-2 payload inside the SpooQy-1 satellite [5]

The payload optical layout is shown in Fig. 1. A 405nm laser beam propagates from the laser diode (Fig. 1-1) through several optical elements/crystals generating polarization-entangled photon pairs by a collinear, non-degenerate type-I Spontaneous Parametric Down Conversion (SPDC) process [5]. The photons in each pair are separated by a dichroic mirror (Fig. 1-10) and detected by separate avalanche photodiodes (Fig. 1-15).

As SPEQS-2 relies on avalanche photodiodes (APDs) for detecting single photons, it is critical to understand the factors that affect the detection count rates. A main effect of radiation damage is an increase in the dark count rate (DCR) at the detectors. This results in a lower signal-to-noise ratio, critical to the feasibility of the technology for Quantum Key distribution (QKD) [6].

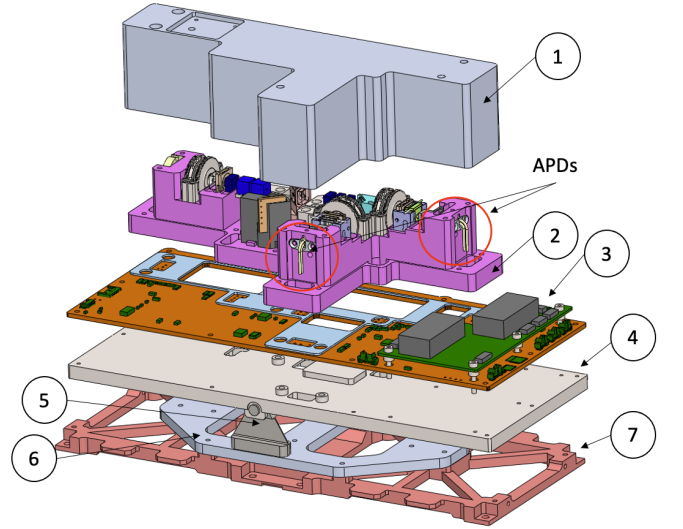


FIG. 2. Exploded view layout: Mechanical assembly of payload on-board SpooQy-1 satellite: (1) Cover for the optical unit, Material - Aluminium (AL6061-T6). (2) Optical unit (Payload): Single Photon Entangling Quantum System (SPEQS-2), Material - Titanium (Ti-6Al-4V). (3) On board electronics mounted onto PCB, Material - FR4). (4) Custom baseplate for the scientific instrument, Material - Titanium (Ti-6Al-4V). (5) Isostatic base mount, Material - Stainless Steel (SS304). (6) Mount base, Material - Aluminum (AL6061-T6). (7) One ribs skeleton, Material - Aluminum (AL7075-T6-2).

Radiation modeling requires understanding of the mechanical layout that acts as radiation shielding materials for critical components. Knowledge of the geometry enables us to assess the effects of differences in shielding materials surrounding the critical components. Fig. 2 shows the exploded view of the payload assembly, depicting the several layers of mechanical components of different materials. The optical elements are integrated into the optical unit (Fig. 2-2), a custom made titanium single block. The onboard electronic board is sandwiched in between the optical unit and the custom baseplate (Titanium). The optical unit is enclosed with an aluminum cover. The isostatic base mount (Stainless steel) and aluminum mount base acts as the structural interface between the payload and skeleton of the satellite.

Section IV further discusses the photodiodes used on the CubeSat and the measured dark count rate collected over 700 days in-orbit from SpooQy-1. Continued radiation damage can increase the dark count rate to a level where quantum devices cannot reliably operate. Single photon detectors are crucial for such free-space space quantum technology applications and radiation damage is of considerable concern and we investigate the use of radiation modelling as a means of predicting radiation induced performance degradation on the SpooQy-1 space mission.

B. Space Radiation

Satellites face environmental hazards such as launch conditions, vacuum, frequent large temperature cycles, and space radiation. Radiation in the form of highly energetic particles (electrons, protons, ions, and neutrons) can damage spacecraft electronics and components. Radiation in Low Earth Orbit (Fig. 3) is mostly due to electrons and protons trapped by the Earth's magnetic field in the Van Allen radiation belt [2]. Their density strongly depends on the inclination and altitude of the satellite's orbit. Since CubeSats are constrained by size, weight, and power, it is crucial to understand the radiation shielding capabilities of various materials and how the space radiation can damage payload instruments.

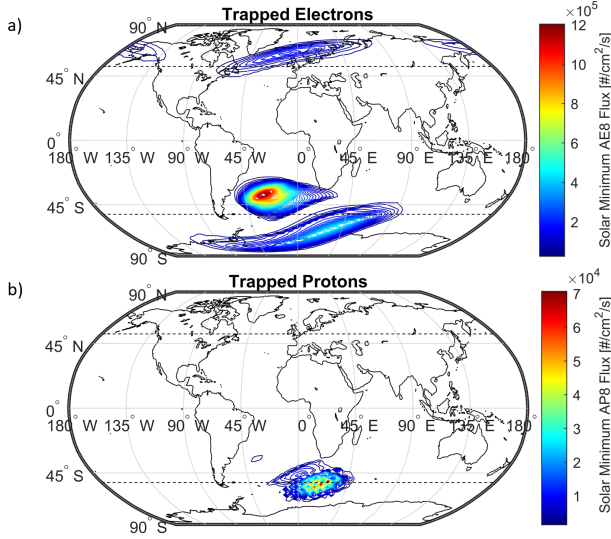


FIG. 3. Abundance of trapped particles regions at 400 km altitude using fluences from SPENVIS [2]. (a) trapped electron population. (b) trapped proton population. The South Atlantic Anomaly (SAA) South East of South America is where particles are most abundant. The SpooQy-1 orbit at 51.6° inclination (between the dashed lines) overlaps with the SAA.

C. Radiation effects on APDs

Charged particles in space radiation deposit energy in materials via several mechanisms which can be ionizing or non-ionizing for the material and result in their degradation [7] [8] [1]. Radiation dose is defined as the amount of energy deposited per unit mass (commonly using rads [0.01 J/kg] or grays [1 J/kg]). Displacement damage is a form of non-ionizing dose resulting in displacement of atoms from lattice positions, radiation testing of Geiger APDs reveal they have high sensitivity to displacement damage with relatively low sensitivity to ionizing radiation. The relationship between displacement damage dose and its induced dark count rates are

shown in Eq. 1 [6]. As the Geiger APDs (SAP500) are not radiation hardened they exhibit part-to-part variability in their response. For the purposes of radiation modelling, we assume there is no part-to-part variability in the displacement damage dose (DDD) induced degradation across the two APDs,

$$\Delta DCR = \frac{V n_i}{2K_{gn}} \cdot \phi, \quad (1)$$

where ΔDCR is the radiation induced dark count rate in counts per second, V is the depletion region volume of the Geiger APD, n_i is the intrinsic carrier density, K_{gn} is the damage coefficient for the material used in the geiger APD, and ϕ is the radiation dose. The intrinsic carrier density is the density of electrons generated in the depletion region [9] [6]. The damage coefficient measures the newly radiation induced bulk generation centers in the depletion region and is independent of temperature. The variables V , n_i , and K_{gn} are constants. With no part-to-part variability, the equation depicts a linear relation between the radiation dose damage and induced dark count rate.

$$\frac{\Delta DCR_1}{\Delta DCR_2} = \frac{\phi_1}{\phi_2} \quad (2)$$

Where ΔDCR is the change in dark count rates observed for a corresponding radiation dose of ϕ . This is further discussed in section IV correlating the simulated data and in-orbit data from SpooQy-1.

III. METHODS

The radiation effects will be simulated using a high fidelity 3-dimensional CAD model of the satellite. Assuming a set of ideal conditions hold;

1. No part-to-part variations in displacement damage induced dark counts
2. Negligible manufacturing inconsistencies with intrinsic carrier density, silicon damage coefficients
3. Identical depletion region volumes for both APDs
4. APDs' dark count rates are more sensitive to displacement dose damage.

Using these set of conditions, we can correlate by Eq. 1 the ratios of dark count rates with the ratios of displacement damage doses of the GM-APDs. The radiation modelling is conducted in RSim [3]. The mission fluences obtained from SPENVIS [2] and the satellite CAD model (along with material Z atomic number and densities) are imported into RSim. The radiation model assumes;

1. No temperature effects
2. No preferential satellite orientation (i.e. an omnidirectional radiation environment)

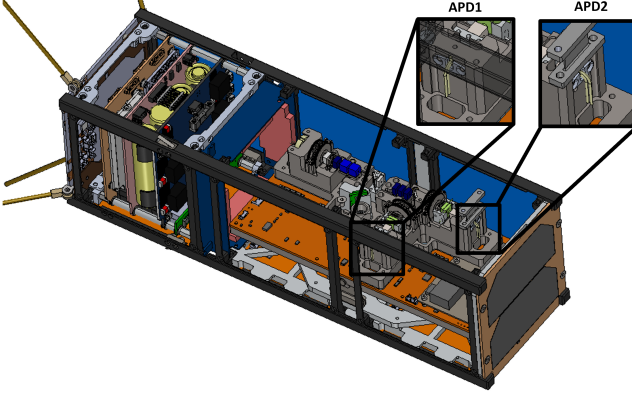


FIG. 4. Locations of the GM-APDs (APD1 and APD2) on-board SpooQy-1. These detectors are surrounded by various components and some have been hidden for better direct visibility of the GM-APDs.

These assumptions are based on telemetry and thermal gradient data obtained from the SpooQy-1 satellite. After 600 days, the increased atmospheric drag may stabilize the satellite's orientation due to the sharp decline in altitude. Also, the data on satellite orientation was unavailable beyond 600 days during the analysis. Hence no radiation modelling is conducted beyond 600 days.

SPENVIS was used to simulate the SpooQy-1 space radiation environment (consisting mainly of electrons and protons, ions are neglected as they have minimal contribution to radiation dose) for 6 mission segments of 100 days (chosen arbitrarily) using orbital data as shown in Fig. 8b. Minimal solar activity is assumed, consistent with the mission date and mission solar activity (mission was during minimum of 25th solar cycle [10]). The particle models used were AP8-MIN, AE8-MIN (97%), SAPPHIRE, and ISO15390 for trapped protons, electrons, solar protons, and cosmic protons, respectively. The SPENVIS orbital parameters for SpooQy-1 were thus set to a trajectory duration of 30 days, orbital inclination of 51.64° , ascending node of 48.59° , and argument of perigee at 67.56° . Prior to simulating all 6 mission segments, a simulation was conducted for constant altitude (408-410 km) for a simplified general radiation exposure analysis for SpooQy-1. Fig. 4 shows the 3D model that is imported into the RSim software for radiation analysis with highlighted locations of the two GM-APDs.

Each particle source was simulated separately with 10,000,000 primary particles and geometric biasing for accurate modelling. Shielding physics with option 4 and 3 for protons and electrons was used, respectively, providing tolerable compromise between computational costs and simulation errors. To facilitate a more detailed understanding of the relation between particle type and energy range, and the corresponding absorbed dose in individual sections and components of the satellite, the radiation dose contributions from various particles and energy bands were simulated. The displacement damage

dose was calculated using the simulated spectral fluences into the GM-APDs using a NIEL calculator [2, 11].

IV. RESULTS AND DISCUSSION

To investigate the use of radiation modelling as a performance predictor for the GM-APDs, we attempt to correlate the simulated displacement damage dose with the observed dark count rates. Assuming the two GM-APDs are identical, this can be achieved using dark count rate and displacement damage dose ratios in Eq. 1.

A. Radiation Simulation Results

First, before simulating the environment in full detail, a simple 1-year radiation model was created for a constant altitude, the radiation dose contributions for the GM-APDs are summarized in table I, and is broken down on a particle energy and type basis.

Particle	Energy [MeV]	APD1 [rads]	APD2 [rads]
Electrons			
Low Energy	0-2	190.9	258.5
Medium Energy	2-3	15.3	25.5
High Energy	3-7	4.9	6.8
Protons			
Low Energy	0-60	21.7	33.6
Medium Energy	60-200	18.0	23.8
High Energy	200-400	3.5	3.8
Extreme Energy	400-100,000	0.001	0.015
Total Dose		254.3	352.0

TABLE I. Radiation dose contribution breakdown for a specific orbit (Altitude: 410km, Inclination: 51.64° , ascending node: 48.59° , mission time: 1 year). Detector doses from averaged omnidirectional particle fluences. For both APDs more than 99% of the dose is from trapped electrons and protons. Uncertainties in the total radiation doses are 5% 9% relative error for protons and electrons, respectively.

From the simulations the contributions from solar protons and galactic cosmic ray protons were found to be negligible as the majority of the dose was from trapped electrons and protons. Moreover, there are varied levels of radiation exposure for the two GM-APDs. This is likely a result of their different positions within the space vessel, and is also seen in the dose deposition heatmap as shown in Fig. 5. The main differences in radiation exposure between the two APDs was seen in primary particles. The hypothesis is that the increased dose observed at APD2 may be due to additional shielding along the payload and satellite, i.e extra radiation dose from high energy particles as they lose energy in the extra shielding, thereby increasing the density of low to medium energy particles

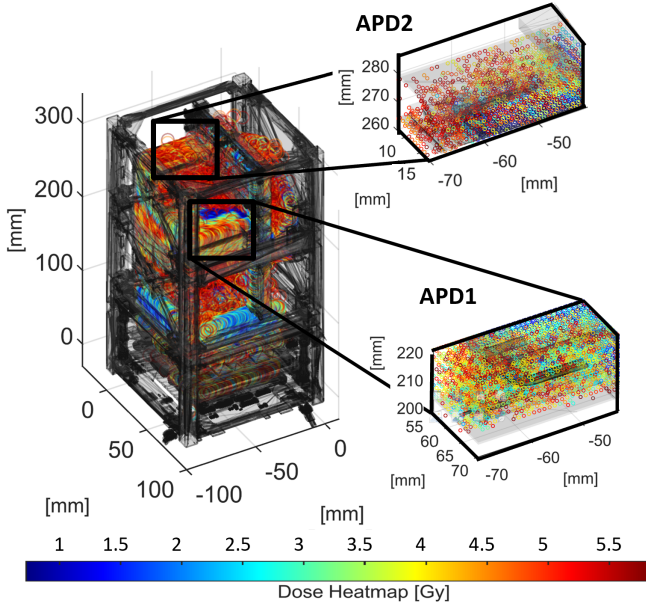


FIG. 5. Heatmap of dose deposits by protons and electrons encountered by the SpooQy-1 CubeSat. With the regions of the GM-APDs named “APD1” and “APD2” highlighted with two views. APD1 is near a dose coldspot and APD2 is more exposed to particles and is in a dose hotspot.

at APD2’s active area. This effect could be significantly enhanced by the shape of the payload into which the GM-APDs were placed, leaving APD2 more exposed to radiation doses from low and medium energy particles. From table I it is also evident that the expected yearly absorbed dose is in the order of 300 rads. As GM-APDs dark count rates are predominantly affected by displacement damage dose (and minimal sensitivity to ionizing dose) [6], the absorbed dose from electrons (mainly ionizing [2]) is expected to have minimal impact on GM-APD performance. The radiation model is further improved by simulating the orbit in full detail by breaking the orbit down into 100 day segments with radiation doses accumulated over time up to 600 days of orbit. Through Fig. 6 the accumulation of DDD and electron radiation dose for the GM-APDs are shown throughout the 600 days of orbit. Using Fig. 6a it is evident that the ratio of displacement damage doses for APD2/APD1 is 1.58 ± 0.31 by the end of the 600 days.

B. Comparison of Simulation Results to In-Orbit Data

The observed dark counts for the GM-APDs onboard SpooQy-1 are shown in Fig. 7a and Fig. 7b for various temperatures with an exponential fitting which are then used to extrapolate a dark count for a normalized temperature of 10 degrees Celsius. The dark count rates as a function of time is plotted in Fig. 7c, and the GM-APD named “APD2” has almost twice the dark count

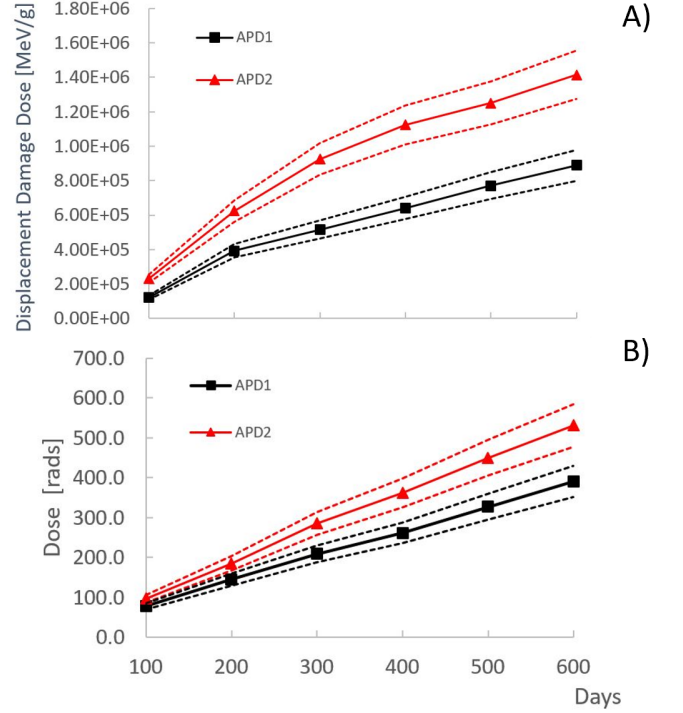


FIG. 6. Simulated accumulated radiation doses over SpooQy-1’s lifetime, A) The simulated accumulation of displacement damage by protons over the mission duration. Note how the trend begins to level off towards the end of the spaceflight. B) accumulation of radiation dose from electrons over time in both GM-APDs. The dashed lines indicate possible values for the radiation dose for the APDs with maximum and minimum limits.

rate compared to “APD1”, the dark count rates increase linearly with orbital days. This linearity is consistent up to 550 days approximately, after which we observe a drop in the slope of the linearity.

It is also important to investigate whether the environmental conditions that the simulations assume are maintained in-orbit, namely i) omnidirectional radiation environment and ii) no part-to-part variability and iii) both GM-APDs operate at the same temperature. The satellite has no preferential orientation, and hence the radiation environment can be assumed to be omnidirectional, the understanding of part-to-part variability requires further radiation testing and research hence cannot be incorporated into the modelling at this time.

Solar exposure can heat the external components of the satellite, and thus heating the SPEQS-2 payload through conductive heat transfer. It is important to eliminate the influence of any thermal gradient across the payload from solar exposure, as temperature can affect the thermally generated electron-hole pairs in the absence of photons leading to increased dark count rates [12]. Fig. 8a shows the maximum thermal gradient across the SPEQS-2 payload, measured from 5 on-board thermistors. The thermal gradient across the SPEQS-2 payload is approx-

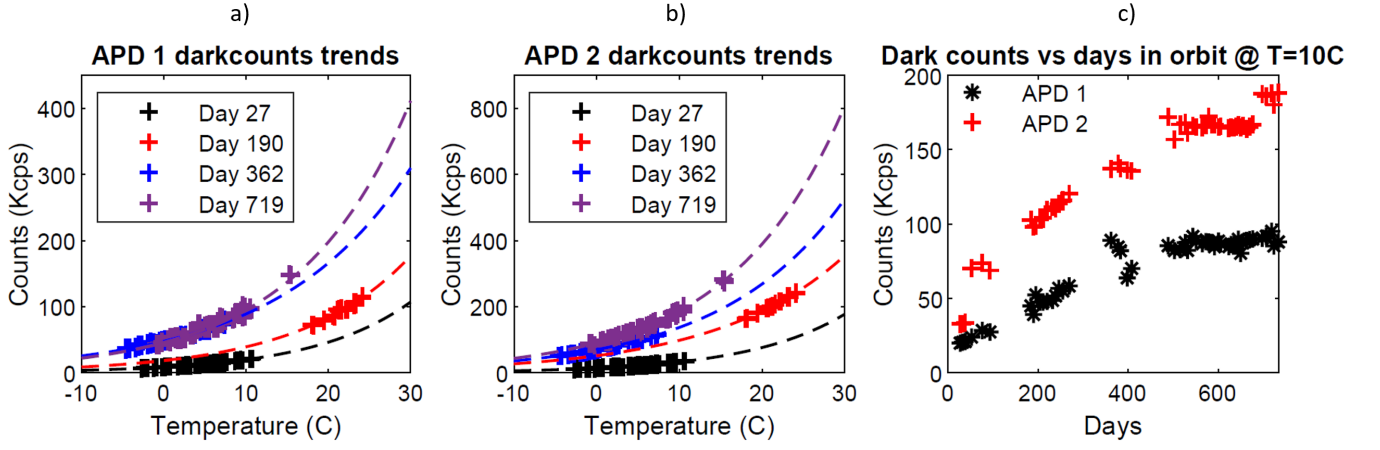


FIG. 7. Dark count rate and temperature measurements for the GM-APDs, APD1 and APD2. (a),(b) - Dark counts recorded over one orbit plotted as a function of its temperature during the measurement for 27, 190, 362, 719 orbital days. (c) - all of the dark count rate measurements normalized to 10°C are shown as a function of time.

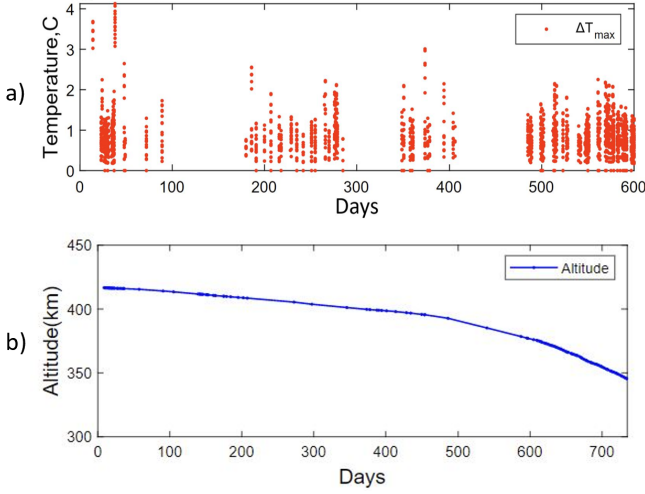


FIG. 8. SpooQy-1's in-orbit data: (a) SpooQy-1's thermal gradient across 5 thermistors on the SPEQS-2 payload over the mission duration (600 days), (b) Plot describing the SpooQy-1's altitude over its mission lifetime

imately 1°C on average through the mission lifetime. Hence temperature variations across the two APDs cannot be responsible for varied dark counts.

However, the increasing dark count rates shows correlation to the satellite's altitude (Fig. 8b). The decline in altitude is found to be steeper from 475 orbital days. It is also observed that the rate of increase in the dark counts is dropped (Fig. 7c) at a similar time frame. This drop in the dark count rates is likely due to the less radiation dose damage observed at lower altitude. This is possible as the trapped particle population within the Van Allen radiation belts is altitude dependent. Moreover, it was shown there is a linear relationship between dark count rates and radiation dose absorbed (Ref Eq-2). It is highlighted that the accumulated displacement

damage dose and dark count rate ratios are only comparable assuming both GM-APDs are identical and have negligible differences in intrinsic carrier density, depletion region volumes, damage coefficients and other GM-APD structural differences are negligible.

Though discrepancy due to part-to-part variations exist in the displacement damage dose tests (conducted at $22 - 25^\circ \text{C}$) as shown in Fig. 11, the in-orbit dark count rates and simulated displacement damage doses are in general agreement. The simulated DDD were $1.41 \cdot 10^6 \text{ MeV/g}$ and $0.89 \cdot 10^6 \text{ MeV/g}$ for APD2 and APD1, respectively, which correspond to 300-400 kcps and 200 kcps for APD2 and APD1, respectively.

Through Fig. 9 we compare the DDD and DCR ratios accumulated over the six mission segments. We observe that the DCR ratio from the measured dark counts seems to agree with the estimated DDD ratios within its margin. The disagreement for the first two segments among the ratios may be a result of a lack of dark count measurements in the first 200 days, part-to-part variability in performance, or possibly that the environmental modelling was not accurate within this time.

Whether high-fidelity radiation modelling can be used as a predictor for radiation induced performance degradation remains an open-ended question as further understanding the mechanisms behind part-to-part variability in radiation damage of APDs is not fully understood and may be result of manufacturing inconsistencies [13]. Improved radiation testing may also narrow the gap between instrument performance during radiation tests and in-orbit performance, the radiation testing of the GM-APDs involved monoenergetic gamma rays proton beams for ionizing and displacement damage doses. Space radiation follows a broadband exponential energy spectra, and as a result radiation testing guidelines recommend using a suite of electron or gamma and proton energies for risk assessments [8]. Using broadband electron beams may also prove beneficial as APD dark counts are also af-

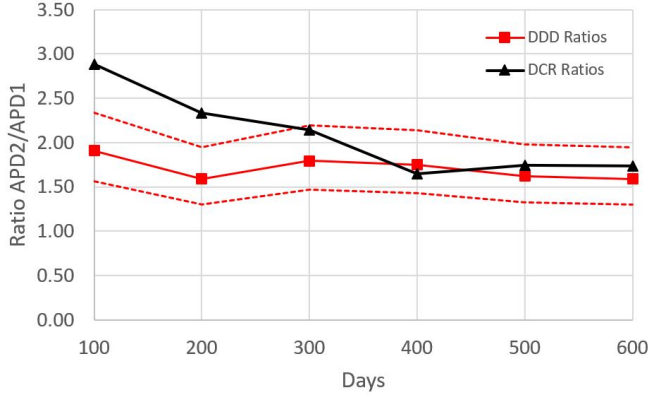


FIG. 9. Comparing the simulated displacement damage dose (DDD) ratios with the observed DCR ratios plotted for six segments of SpooQy-1's orbital lifetime.

ected by charge trapping of low energy electrons which are non-ionizing [14]. For this purpose using laser plasma accelerators [15] may prove beneficial as they are capable of producing broadband exponential energy electron and proton beams.

V. CONCLUSION

Here, we described the mission-level objective of the SpooQy-1 mission and a critical component in the payload, GM-APD. The mechanical layout of the payload is described (Fig. 4) with the geometrical placement of the two GM-APD and their shielding materials. Further, the radiation-induced dark counts of the APDs are represented as a function of their radiation level exposure (Eq. 1). Analysis of the collected dark count data over the orbital lifetime shows that the drop in the increasing dark count rate after 500 days correlates to the steep decline in the altitude (Figs 7-8). This indicates that the change in the dark counts measured may be due to radiation-induced. The APDs' radiation dose level is assessed through high-fidelity radiation modelling techniques, which incorporate the orbital parameters (trapped particle fluence data, altitude) into the Cube-Sat's CAD model (Section III). The mission-level radiation doses are then correlated with in-orbit dark count data. Despite the part-to-part variability assumption in displacement damage induced dark counts in the GM-APDs, the correlation still agrees for the most of the mission. Under ideal conditions, assuming no differences in structural, material, manufacturing inconsistencies, and that an omnidirectional radiation environment is maintained, the GM-APDs dark count rate ratios would likely be within the expected performance boundaries shown in Fig. 9.

This study presents an approach to estimating the radiation dose damage for a critical payload component through high-fidelity radiation modelling techniques us-

ing the CAD model. This complements data obtainable from radiation testing. For an effective in-orbit radiation damages assessment, the radiation effects of the components must be understood. Hence, with multiple iterations this approach enables us to optimize the structural design and shielding material for a critical component, thus increasing its operational lifetime.

ACKNOWLEDGMENTS

DO acknowledges support from the EPSRC Researchers in Residence at the Satellite Applications Catapult (EPSRC Grant Ref: EP/T517288/1). DO and ALenart acknowledges support from the International Network in Space Quantum Technologies (EP/W027011/1) and the EPSRC Quantum Technology Hub in Quantum Communication (EP/T001011/1). ALenart acknowledges the support of an EPSRC Doctoral Training Partnership award. ALing acknowledges the support from the National Research Foundation, Singapore, under its Central Gap Fund (Ref: NRF2018NRF001-001).

VI. APPENDIX

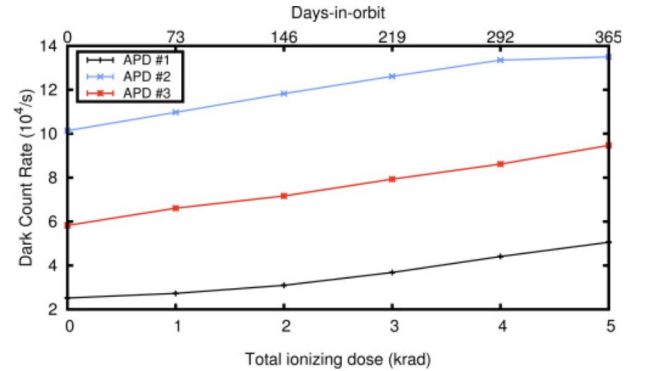


FIG. 10. DCR vs Ionising Dose. The dark count rates are also induced by ionizing radiation (where electrons are main contributor). The radiation tests were conducted by the National University of Singapore [16]. A separate batch of three GM-APD (SAP500) devices were used for ionizing radiation tests using a Cobalt-60 gamma ray radiation chamber. The SAP500 manufacturing standards limits the initial dark count rate to be anywhere within 15000 s^{-1} [12], the radiation induced dark count rates are measured from this point.

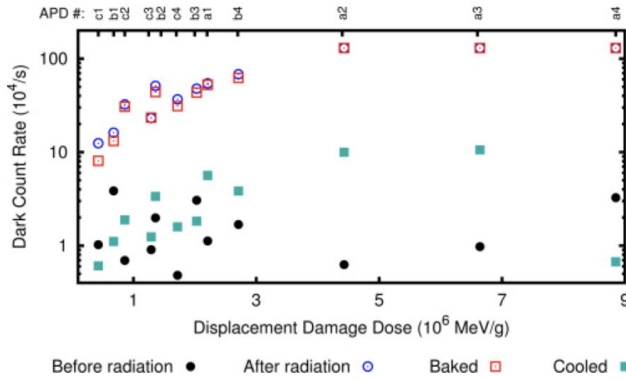


FIG. 11. DCR vs Displacement Damage Dose. A correlation between sustained displacement damage dose and dark count rates for the GM-APDs can be observed. The radiation tests were conducted by Crocker Nuclear Laboratory [16] for 12 GM-APD devices with different proton energies (group a : 5 MeV, b : 25 MeV, c : 50 MeV) and 4 different total proton fluences were used for each group.

- [1] Campola, M. J. & Pellish, J. A. Radiation hardness assurance: Evolving for newspace. In *European Conference on Radiation Effects on Components and Systems (RADECS 2019)*, GSFC-E-DAA-TN72757 (2019).
- [2] (project manager), E. D. D., Messios, N., Calders, S., Calegaro, A. & Mezhoud, S. Space environment information system (2021). URL <https://www.spenvis.oma.be/help/background/traprad/traprad.html>. <https://www.spenvis.oma.be/>.
- [3] Tech-X Corporation. RSim (2021). URL [\url{https://txcorp.com/rsim/}](https://txcorp.com/rsim/).
- [4] Agostinelli, S. & et. al. Geant4—a simulation toolkit. *Nuclear Instruments and Methods in Physics Research Section A: Accelerators, Spectrometers, Detectors and Associated Equipment* **506**, 250–303 (2003). URL <https://www.sciencedirect.com/science/article/pii/S0168900203013688>.
- [5] Villar, A. *et al.* Entanglement demonstration on board a nano-satellite. *Optica* **7**, 734–737 (2020). URL <http://opg.optica.org/optica/abstract.cfm?URI=optica-7-7-734>.
- [6] Yang, M. *et al.* Spaceborne, low-noise, single-photon detection for satellite-based quantum communications. *Optics express* **27**, 36114–36128 (2019).
- [7] Grimes, D. R., Warren, D. R. & Partridge, M. An approximate analytical solution of the bethe equation for charged particles in the radiotherapeutic energy range. *Nature* **7** (2017). URL <https://doi.org/10.1038/s41598-017-10554-0>.
- [8] Buchner, S., Marshall, P., Kniffin, S. & LaBel, K. Proton test guideline development—lessons learned. *NASA/Goddard Space Flight Center, NEPP* (2002).
- [9] Privitera, S. *et al.* Towards a new concept of photomultiplier based on silicon technology (2007).
- [10] NOAA Space Weather Prediction Center. Solar Cycle Progression — NOAA / NWS Space Weather Prediction Center. URL <https://www.swpc.noaa.gov/products/solar-cycle-progression>.
- [11] Boschini, M., Rancoita, P. & Tacconi, M. Total niel dose calculator for spectral fluence (2020). URL <http://www.sr-niel.org/index.php/sr-niel-web-calculators/niel-dose-calculator-for-spectral-fluence-of-electrons-protons-and-ions>.
- [12] Laser Components. Silicon geiger mode avalanche photodiode (2020). URL https://www.lasercomponents.com/de/?embedded=1&file=fileadmin/user_upload/home/Datasheets/lc-apd/sap-series.pdf&no.cache=1.
- [13] Becker, H., Miyahira, T. & Johnston, A. The influence of structural characteristics on the response of silicon avalanche photodiodes to proton irradiation. *IEEE Transactions on Nuclear Science* **50**, 1974–1981 (2003).
- [14] Kawauchi, T., Wilde, M., Fukutani, K., Okano, T. & Kishimoto, S. Effect of electron irradiation dose on the performance of avalanche photodiode electron detectors. *Journal of Applied Physics* **105**, 014506 – 014506 (2009).
- [15] Hidding, B. *et al.* Laser-plasma-accelerators—a novel, versatile tool for space radiation studies. *Nuclear Instruments and Methods in Physics Research Section A: Accelerators, Spectrometers, Detectors and Associated Equipment* **636**, 31–40 (2011).
- [16] Tan, Y. C., Chandrasekara, R., Cheng, C. & Ling, A. Silicon avalanche photodiode operation and lifetime analysis for small satellites. *Opt. Express* **21**, 16946–16954 (2013). URL <http://www.opticsexpress.org/abstract.cfm?URI=oe-21-14-16946>.